LLNL-TR-666388

LAWRENCE
LIVERMORE
NATIONAL
LABORATORY

The Development of DYNA3D Material Model 67 - Hyperelastic Elastomeric Foam With Viscoelasticity

E. Zywicz

January 21, 2015

This work performed under the auspices of the U.S. Department of Energy by Lawrence Livermore National Laboratory under Contract DE-AC52-07NA27344.

The Development of DYNA3D Material Model 67 - Hyperelastic Elastomeric Foam With Viscoelasticity

Edward Zywicz
Methods Development Group
Defense Technologies Engineering Division
Engineering Directorate

February 20, 2015

Summary

A strain energy potential is developed to represent isotropic, medium-density, elastomeric foams under predominately compressive volumetric states. The potential is proven to be polyconvex and coercive, and is thus stable for all admissible loadings. The potential includes terms that capture the increase in hydrostatic and deviatoric stiffnesses as the relative volume decreases to and slightly beyond full consolidation, i.e., the phenomenon commonly called "lock-up". The model is shown to accurately replicate the axial compressive stress and secant shear modulus from combined uni-axial stress/torsion experiments. An appropriate viscoelastic formulation for the potential is summarized. The potential and viscoelastic option are implemented in the explicit finite element code DYNA3D (Zywicz and Lin, 2014) as material model 67.

1 INTRODUCTION

Polymer-based elastomeric foams are used in many applications, and their mechanical behavior and properties have received much attention (see e.g., Gibson and Ashby, 1977). The mechanical response of medium-density foams, those with relative densities between 0.1 and 0.9, is often idealize in the same manner as low-density foam. This includes hyperelastic potentials and phenomenological based models. The difficulty with both approaches is they are often only accurate and stable for a subset of deformations that commonly exclude volumetric states near full consolidation, *i.e.*, lock-up. Surprisingly, few micro-mechanically based hyperelastic formulations have been developed for medium-density foams.

Danielsson, Parks, and Boyce (2004) developed a hyperelastic constitutive relationship for porous elastomeric media. The micro-mechanically based model is based upon a hollow incompressible Neo-Hookean sphere subjected to a kinematically admissible displacement field. The system energy is calculated in terms of imposed macro strain invariants and then normalized by the system volume. The resultant strain energy potential is defined in terms of the matrix material Neo-Hookean parameter, the initial void volume fraction, and two macro strain invariants. The model yields initial shear and bulk moduli that are in agreement with other micro-mechanical based approaches. The constitutive relationship predicts that the deviatoric and volumetric stiffnesses increase non-linearly as the relative volume decreases consistent with experimental observations and detailed finite element simulations. Lewis (2005) independently developed a similar constitutive model with a Mooney-Rivlin matrix idealization. Although the derivation utilized a different kinematic formulation, the resulting constitutive model is identical to that of Danielsson *et al*. when only the Neo-Hookean terms are retained.

The Danielsson *et al*. potential has several shortcomings. The potential contains a singularity when the relative volume reaches lock-up that causes an infinite bulk modulus. For truly incompressible materials, this is reasonable. However, this renders the potential inappropriate for modeling foams with slightly compressible matrix material near and beyond lock-up - which is the focus of this model. For initial void volume fractions greater than about 0.7, the potential is not polyconvex and thus may generate non-real wave speeds in this regime. Furthermore, the potential does not replicate the initial linear and plateau region responses normally observed in uni-axial and volumetric compression and appears to overpredict how much the shear stiffness increases with compression, especially near lock-up. (Note, this model was developed for tensile volumetric loadings, and the later deficiencies pertain to compressive volumetric states.) Unfortunately, neither the potential nor formulation easily lends themselves to the inclusion of a compressible matrix.

The goal of the present work is to develop a hyperelastic constitutive model for medium density foams subjected to combined compression and shear for use in numerical calculations. The loading condition of primary interest resembles plane strain compression with small, superimposed transvers shears. The model needs to accurately represent the axial stress and transverse shear stresses for relative volumes from $1\text{-}f_o/3$ to slightly beyond lock-up ($1\text{-}f_o$). Here f_o denotes the initial void volume fraction of the foam.

This report is organized as follows. Section 2 discusses stability and related requirements for strain energy potentials. In section 3, the proposed strain energy function is presented and its stability, i.e., polyconvexity, is proven. A viscoelastic formulation appropriate for the proposed hyperelastic potential is summarized in Section 4. Section 5 describes the experimental data that motivated this potential and shows the ability of the current potential to replicate the desired behavior. In Appendix A, the polyconvexity of several strain energy terms are evaluated in detail.

2 STABILITY REQUIREMENTS

In order to yield unique solutions in elasto-static and elasto-dynamic problems, various requirements are imposed on strain energy potentials. Potentials should represent the material stress-free in its natural state and the value of the potentials should approach ∞

as $J \to 0^{+}$ and as $J \to \infty$, where J is the determinate of the deformation gradient **F**. Most importantly, the potential must be "stable".

Drucker stability (e.g., Drucker, 1959), as applied to hyperelastic materials, requires that the material tangent stiffness matrix, based on the Kirchhoff stress and logarithmic strain, be symmetric and positive definite. This point-wise requirement ensures that the acoustic tensor is positive definite, i.e., yields real wave speeds, and that the governing differential equations remain elliptical. A potential need only satisfy this requirement for deformations of interest. For isotropic materials, the range of stability for a specific potential can normally be identified *a priori* and curve-fitted parameters can be modified to alter the stable range.

Polyconvexity (Ball, 1977) is a stronger requirement than Drucker stability. Strain energy potentials that satisfy the polyconvexity condition guarantee ellipticity and, when combined with coercivity, ensure the existence of minimizers. Polyconvexity requires that the strain energy density function be definable in terms of **F**, *Adj* **F**, and *Det* (**F**) (=*J*), where *Adj* denotes the adjugate of **F** (=J$\mathbf{F}^{-1}$) (Schroder and Neff, 2002). The function must be convex over its entire admissible domain with respect to the nineteen primary variables, i.e., *J* and the components of **F** and *Adj* **F**. By convex, it is meant that the Hessian matrix is positive semi-definite for all admissible **F**. For isotropic materials, it is sufficient to define the potential in terms of the regular or isochoric strain invariants of the right (***C***) or left (***B***) Cauchy-Green deformation tensors since these invariants can be written in terms of **F** as $I_1 = \|\mathbf{F}\|^2$, $I_2 = \|Adj\,\mathbf{F}\|^2$, $I_3 = \left(Det\left(\mathbf{F}\right)\right)^2$, $\overline{I}_1 = \|\mathbf{F}\|^2 \big/ \left(Det\left(\mathbf{F}\right)\right)^{2/3}$, and $\overline{I}_2 = \|Adj\,\mathbf{F}\|^2 \big/ \left(Det\left(\mathbf{F}\right)\right)^{4/3}$ (Hartmann and Neff, 2003). To determine if an isotropic potential expressed in terms of the strain invariants is convex, the Hessian is calculated with respect to the independent variables $\|\mathbf{F}\|$, $\|Adj\,\mathbf{F}\|$, and *J*, as appropriate, and examined to see if it is positive semi-definite. For potentials with just one independent variable, polyconvexity requires the second derivative be non-negative. Polyconvex potentials possess the added benefit that when summed the resultant potential is also polyconvex.

Coercivity pertains to how functions behave as their arguments tend toward large, in magnitude, values. The coercivity condition for strain energy potentials is expressed as an inequality as

$$W\left(\mathbf{F}\right) \geq \alpha\left(\|\mathbf{F}\|^{p} + \|Adj\,\mathbf{F}\|^{q} + \left(Det\left(\mathbf{F}\right)\right)^{r}\right) + \beta$$

with $\alpha > 0$, $\beta \geq 0$, $p \geq 2$, $q \geq p/p-1$, and $r > 1$ (Ebbing, 2010). If admissible values for the associated terms can be found, then the potential is coercive. For potentials that are sums of positive terms, the entire potential is coercive if one or more term is coercive.

Convexity of a strain energy potential is a stronger and generally harder to prove requirement than polyconvexity. Convexity requires the Hessian matrix of the potential to be positive (semi-) definite for all admissible **F**. Here, the independent variables are the nine components of **F**. Potentials that are convex (in the convexity sense) are also polyconvex although the opposite is not necessarily true. Unfortunately, convexity precludes certain desirable physical requirements and functional forms. For example, the term *Det(**H**)* is not convex and therefore terms that are function of only J are never convex.

In practical application, non-polyconvex potentials that satisfy Drucker stability in only limited domains are often used in numerical calculations. For example, the Odgen potential is polyconvex provided its coefficients satisfy certain requirements. When the potential is curve fit to experimental data, coefficients sometimes arise that violate these requirements but improve the fit in certain stretch regions. Although the resultant potential is not polyconvex, it often satisfies Drucker stability for certain deformation regimes and is useful nonetheless.

For the purposes herein, acceptable strain energy potentials are limited to those that are polyconvex and coercive. For additional discussion on convexity, polyconvexity, coercivity, and related topics see, e.g., Ebbing (2010), Hartmann and Neff (2003), and Schroder and Neff (2002).

3 STRAIN ENERGY POTENTIAL

The proposed strain energy potential is given by

$$W = A_0\left(J-1-A_1\ln\left(1+\frac{J-1}{A_1}\right)\right)H_1\left(J-J'\right)+A_2'\left(\frac{J}{A_3}-1-\ln\left(\frac{J}{A_3}\right)\right)H_2\left(J'-J\right)$$
$$+B_0\left(1-J+\frac{1}{B_1}\left(\exp\left(B_1\left(J-1\right)\right)-1\right)\right)+C_0\frac{\left(\bar{I}_1-3\right)^{C_1}}{J^{C_2}}+D_0\left(\bar{I}_1-3\right)$$

where

$$A_2' = A_2\left(1-A_1\right)^2,$$

$$H_1(x)=\begin{cases}0 & x<0\\ 1 & x\geq 0\end{cases} \quad \text{and} \quad H_2(x)=\begin{cases}0 & x\leq 0\\ 1 & x>0\end{cases},$$

$$J' = \left(1-A_1\right)\frac{A_2'+\sqrt{A_0A_1A_2'}}{A_2'-A_0A_1},$$

and

$$A_3 = \frac{A_2'J'\left(1-A_1-J'\right)}{A_0J'(1-J')+A_2'\left(1-A_1-J'\right)}.$$

For this potential, the Cauchy pressure p is given by

$$-p=\frac{\partial W}{\partial J}=A_0\left(1-\frac{1}{\left(1+\frac{J-1}{A_1}\right)}\right)H_1\left(J-J'\right)+A_2'\left(\frac{1}{A_3}-\frac{1}{J}\right)H_2\left(J'-J\right)$$
$$+B_0\left(\exp\left(B_1\left(J-1\right)\right)-1\right)+C_0C_2\frac{\left(\bar{I}_1-3\right)^{C_1}}{J^{C_2+1}}.$$

The A_0 term in the potential causes the pressure to increase rapidly as $J\to\left(1-A_3\right)^+$, where $1-A_3$ is the relative volume at lock-up, and A_3 is approximately the initial void volume fraction. The A_2' term represents the bulk response of the fully consolidated material and is based on the polyconvex volumetric strain energy potential $K\left(\hat{J}-1-\ln\left(\hat{J}\right)\right)$ (Miehe, 1994). The A_2' term is formed by using a multiplicative representation of the relative volume and by assuming the fully dense material is "stress free" when $J=A_3$. This leads to the expression $J=\hat{J}A_3$ or, alternatively, $\hat{J}=J/A_3$. The quantity A_2 has been defined such that it represents the bulk modulus of the fully dense matrix material when $J\approx 1-A_3$. The variables J' and A_3 are constructed such that the pressure and its derivative are continuous at $J=J'$ with respect to the A_0 and the A_2' terms. This results in $1-A_1<J'<A_3$. The B_0 term replicates the initial load up and constant plateau region observed in uni-axial and hydrostatic compression tests, and the value of B_0 is the plateau stress. The D_0 incompressible Neo-Hookean term provides the baseline deviatoric stiffness and, while not obvious, is partially responsible for the increase in the apparent shear modulus with hydrostatic compression. The initial shear modulus is $2D_0$. Lastly, the C_0 coupling term provides additional deviatoric and hydrostatic stiffness. It is responsible for most of the increase in the secant shear modulus with hydrostatic compression. All parameters in the potential are required to be non-negative, and C_1 and C_2 must satisfy the requirements identified in Appendix A.

The polyconvexity of the potential is now examined term by term. The second derivatives of the A_0, A_2', and B_0 terms are

$$\frac{\partial^2\varphi_{A_0}}{\partial J^2}=\frac{A_0}{A_1}\frac{1}{\left(1+\frac{J-1}{A_1}\right)^2}H_1\left(J-J'\right),$$

$$\frac{\partial\varphi_{A_2'}}{\partial J^2}=\frac{A_2'}{J^2}H_2\left(J'-J\right),$$

and

$$\frac{\partial^2\varphi_{B_0}}{\partial J^2}=B_0B_1\exp\left(B_1\left(J-1\right)\right),$$

respectively. As evident, the derivatives are non-negative for all J and therefore these terms are convex and thus polyconvex. The C_0 term is examined in depth in Appendix A and is shown to be polyconvex subject to constraints on C_1 and C_2. (A conservative representation of the constraints are $C_1 \geq 1 + C_2$ and $C_2 \geq 0$.) The compressible Neo-Hookean term associated with D_0 is polyconvex (Hartman and Neff, 2003) and coercive (e.g., Ebbing, 2010). Hence, the entire potential is coercive. Since each term in the potential is polyconvex, the entire potential is polyconvex. Lastly, the potential satisfies the goal that $W \to \infty$ as $J \to 0^+$ and, when $A_0 > B_0$, $J \to \infty$.

4 VISCOELASTIC FORMULATION

A general viscoelastic formulation for hyperelastic materials is presented in Simo and Hughes (1998) – see section 10.5.1. In it, the 2nd Piola-Kirchhoff stress tensor $\boldsymbol{S}$ is defined in terms of a convolution integral (Simo and Hughes, 1998) as

$$\boldsymbol{S}(t) = 2\frac{\partial W_e\left(\mathbf{F}(t)\right)}{\partial \boldsymbol{C}(t)} + \int_{-\infty}^{t} g\left(t-s\right)\frac{d}{ds}\left(2\frac{\partial W_v\left(\mathbf{F}(s)\right)}{\partial \boldsymbol{C}\left(s\right)}\right)ds\,,$$

where W_e and W_v designate the parts of the strain energy potential with and without viscoelastic behavior, respectively. The normalized relaxation function is represented by the Prony-series like expression

$$g(t) = \gamma_\infty + \sum_{i=1}^{N}\gamma_i \exp\left(-t/\tau_i\right),$$

where

$$\gamma_\infty + \sum_{i=1}^{N}\gamma_i = 1\,.$$

For each term in the relaxation function, there is a corresponding internal variable tensor $\boldsymbol{H}^i$. The stress and internal variables are updated using the recursion formulae

$$\boldsymbol{S}_{n+1} = \boldsymbol{S}^0_{n+1} + \sum_{i=1}^{N}\gamma_i \boldsymbol{H}^i_{n+1}$$

and

$$\boldsymbol{H}^i_{n+1} = \exp\left(\frac{-\Delta t}{\tau_i}\right)\boldsymbol{H}^i_n + \exp\left(\frac{-\Delta t}{2\tau_i}\right)\left(\boldsymbol{S}^0_{n+1} - \boldsymbol{S}^0_n\right),$$

where $\boldsymbol{S}^0 = 2\,\partial W_v/\partial \boldsymbol{C}$. The 2nd Piola-Kirchhoff stress is related to the Cauchy stress in the usual manner.

Simo and Hughes (1998) included only deviatoric viscoelasticity in their original presentation. As it is unclear what components behave viscoelastically in an elastomeric foam, the above convolution integral incorporates viscoelasticity on a term-by-term basis. Since the pressure is dominated by the A_0, A_2', and B_0 terms in the potential, this approach provides an easy way to select which components behave viscoelastically.

5 FIT TO EXPERIMENTAL DATA

The current potential is motivated by experimental results for an elastomeric foam with a nominal sixty-five percent initial void volume fraction. The foam was tested in a uni-axial strain experiment and a combined uni-axial stress/torsion experiment. In the combined test, a thin ring was axially compressed to different stretch levels and then torsionally sheared to seven or fifteen percent transvers strain. An axial stress-stretch curve, which extended into the lock-up region, was extracted from the force-displacement data collected in the uni-axial strain test assuming the deformation in the specimen was homogeneous. A secant shear modulus verses axial stretch curve was extracted from the combined stress/torsion experiment at the maximum shear strain level. The analysis of the test assumed the deformation in the specimen, prior to the imposed rotation, was that of uni-axial strain and that the effective shear modulus did not vary with radial position. This allowed the axial stress to be determined as a function of the axial stretch and the secant shear modulus to be determined as a function of the axial stretch and the shear strain level. (For shear strains between one and fifteen percent, the secant shear modulus was observed to be nearly constant.) The axial stress vs. stretch curves obtained from the two experiments were in good agreement over approximately eighty-five percent of their range, but diverged, as expected, near lock-up due to non-homogeneous deformation in the uni-axial stress experiment. Based upon this agreement, it is assumed that the secant shear modulus values are reliable for compressions up to approximately the same level ($J \approx 0.45$).

The axial stress, the transverse stress, and secant shear modulus were calculated for the current potential as a function of the axial stretch. The deformation was assumed to be uni-axial strain prior to the imposition of shear. The potential coefficients were curve fit by matching the axial stress and secant modulus data. The overall fit was evaluated along with the predicted transverse stress. Although no transverse stress data existed, it was assumed that the response should mirror that of the axial response, but with a smaller magnitude indicative of a material with a nearly zero Poisson's ratio. The curve fit process used a least-squares fit based on percent error. The axial response and the two shear modulus fits were weighted so each contributed equally to the error metric.

The value of A_2 was obtained from a separate experiment that used a fully dense sample of the matrix material to measure the bulk modulus. Consequently, the A_2 term was not included in the curve fit process; this was accomplished by setting J' equal to zero.

The predicted results, based upon the curve fit parameters, show very good agreement with the shear modulus and the axial response for all compressive stretch levels as apparent from Figures 1 and 2. Unfortunately, with these coefficient values the transverse stress does not behave monotonically with imposed axial compression but actually becomes tensile for a period prior to lock-up as evident in Figure 3. It was found that if the predicted shear modulus values were lower near lock-up, the transverse stress would behave as desired. Given the questions regarding the analysis of the combined uni-axial stress/torsion experiments in this region, discounting the shear modulus values near lock-up seemed reasonable.

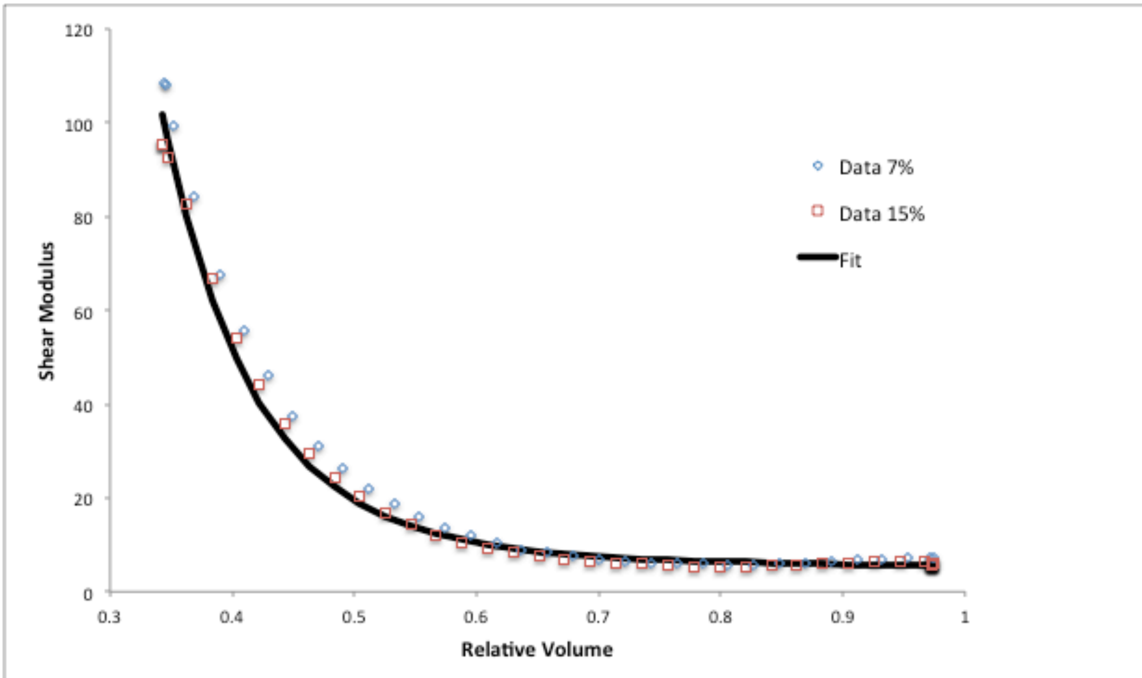

Figure 1 – Fitted and experimental secant shear modulus vs. relative volume

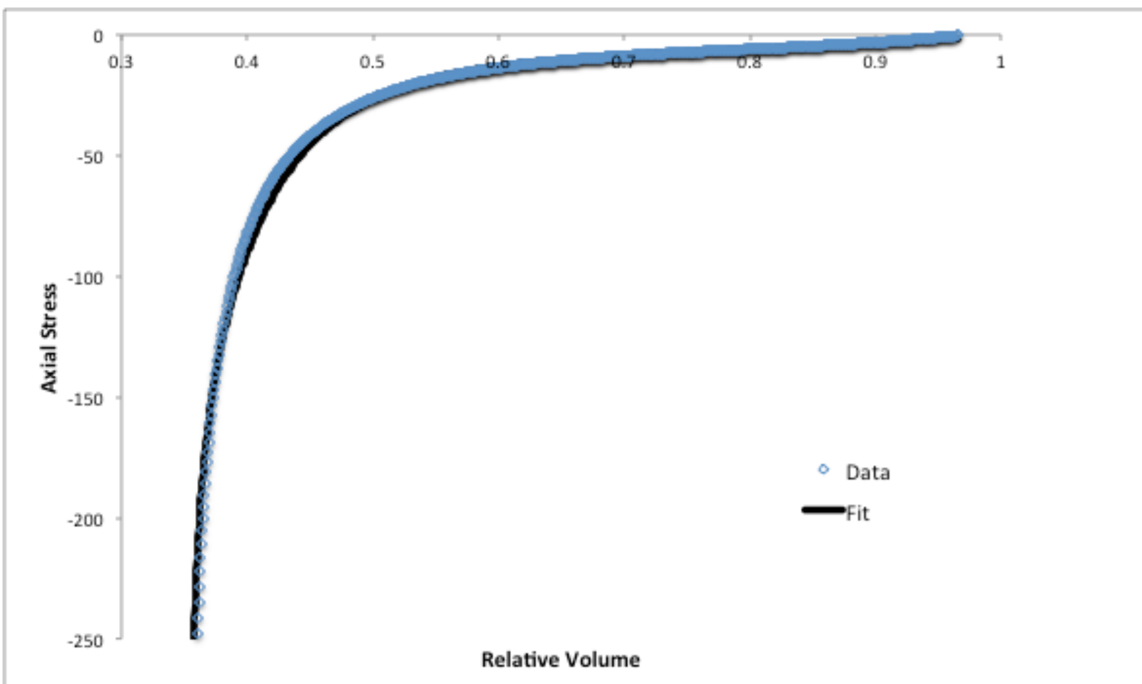

Figure 2 – Fitted and experimental axial stress vs. relative volume

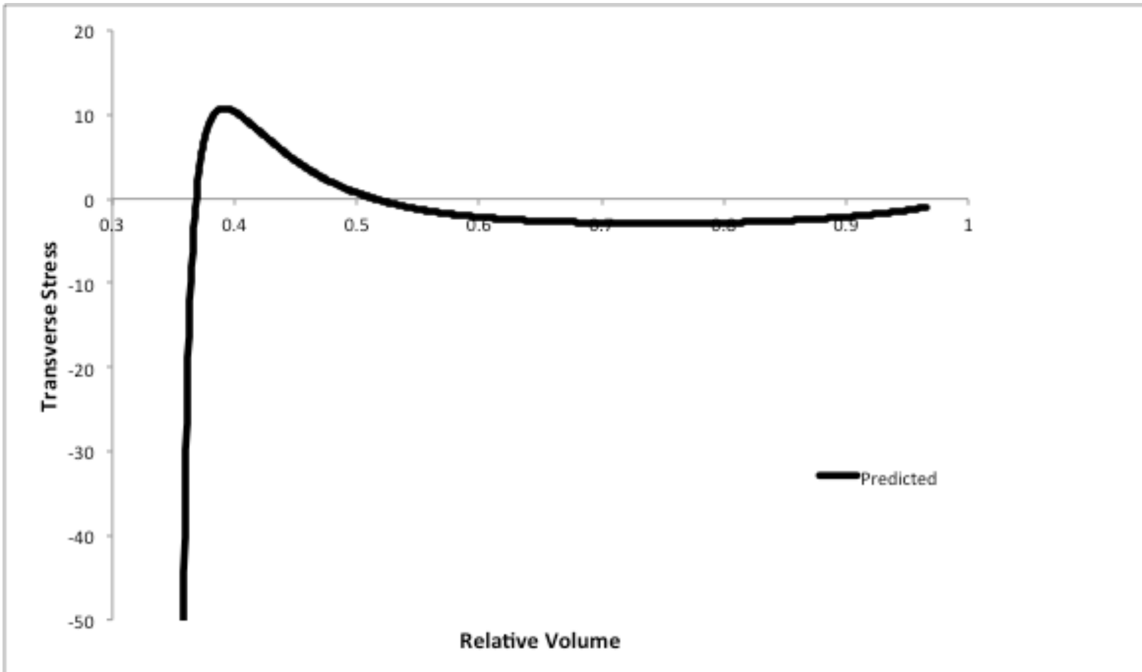

Figure 3 – Predicted transverse stress vs. relative volume

A modified curve fitting process was developed that used the C_0, C_1, and C_2 values obtained from the original curve fit. With C_1 and C_2 fixed, the original C_0 value was reduced and the remaining parameters were obtained via the least-squares fit. The C_0 value was incrementally decreased until the model generated a transverse stress that behaved monotonically. For the current set of data, this amounted to a twelve percent reduction in C_0. Agreement between the shear modulus and axial stress was not significantly impacted as can be seen in Figures 4 and 5. While the largest differences for the shear modulus occur at lock-up, the axial stress demonstrates good agreement at lock-up but reduced agreement at slightly smaller compression levels. This is not surprising since the A_0 term dominates the axial stress near lock-up and the shear modulus does not depend upon it. Figure 6 shows the predicted transverse stress response with the modified coefficients. As desired, the behavior is monotonic.

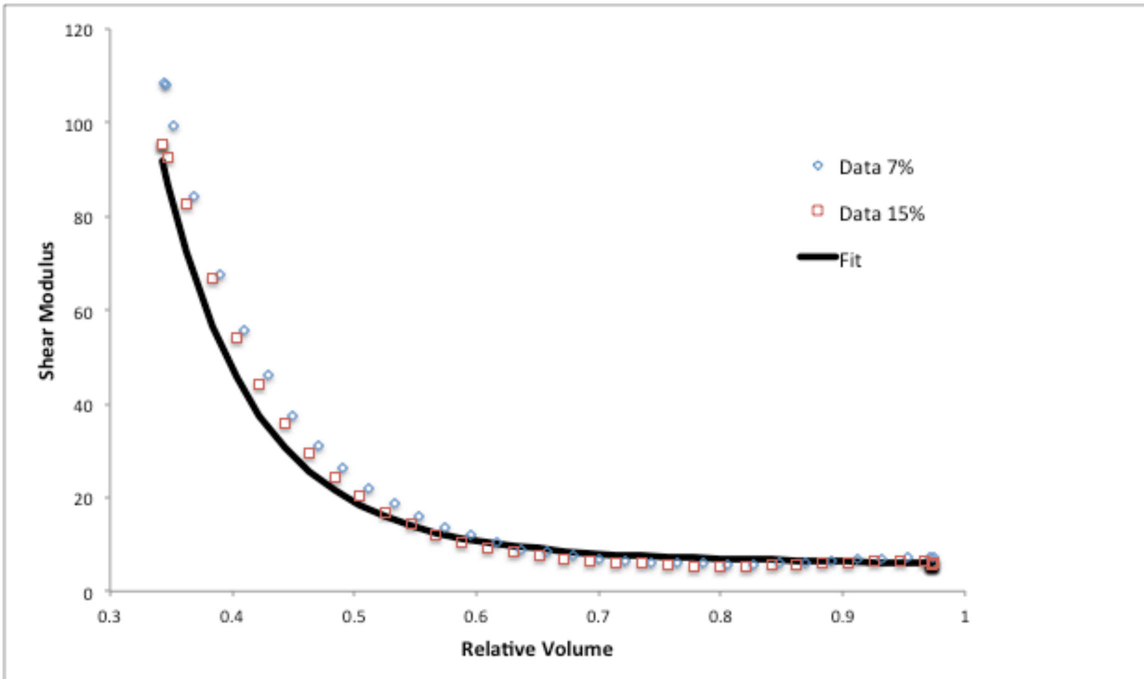

Figure 4 – Fitted and experimental secant shear modulus vs. relative volume with modified coefficients

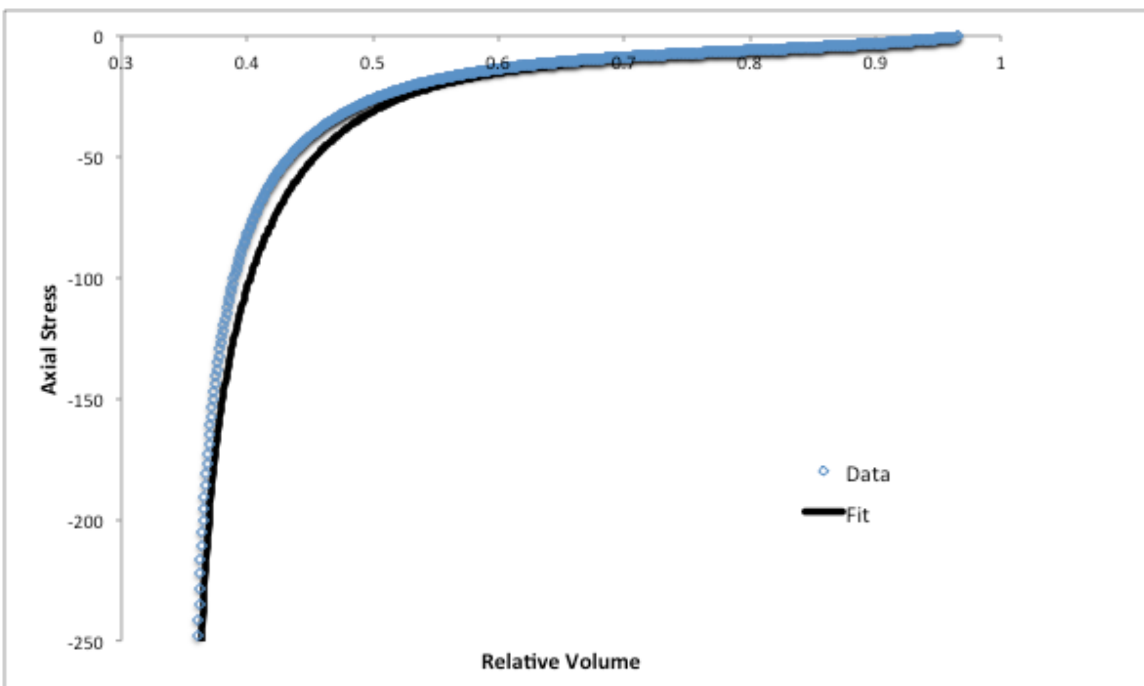

Figure 5 – Fitted and experimental axial stress vs. relative volume with modified coefficients

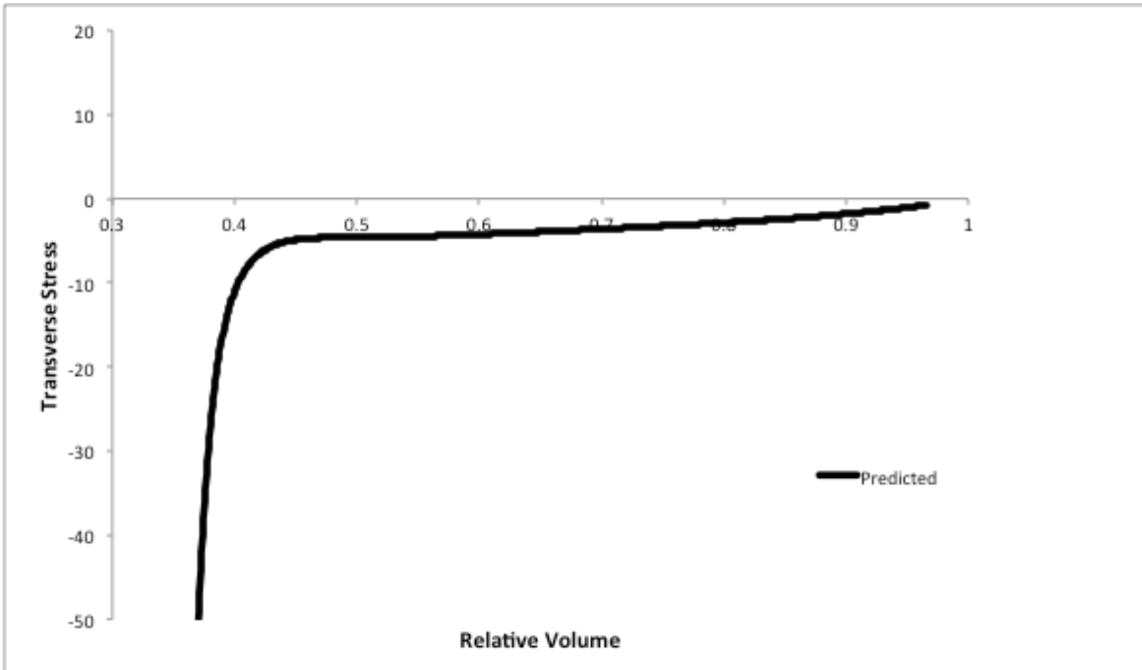

Figure 6 – Predicted transverse stress vs. relative volume with modified coefficients

6 DISCUSSION

A strain energy potential appropriate for medium density, isotropic, elastomeric foams under primarily compressive conditions was assembled. The individual volumetric terms represent the initial ramp up and plateau region, the rapid stiffening region prior to lock-up, and the bulk response in the fully consolidated region. The Neo-Hookean term provides the model with its baseline deviatoric stiffness. The coupling term causes the apparent shear modulus to increase with volumetric compression, beyond that due to the Neo-Hookean term. The potential was proven to be polyconvex and coercive. It is therefore stable for all admissible deformation states, and a minimizer exists for boundary value problems that use it. The potential and an accompanying viscoelastic option were implemented in the explicit finite element code DYNA3D (Zywicz and Lin, 2014) as material model 67.

The model was curve fit to experimental data obtained from a uni-axial strain experiment and from a combined uni-axial stress with torsion experiment. The shear modulus data was extracted from the combined compression/torsion experiment by assuming the deformation prior to the imposition of torsion was that of uni-axial strain. When the best-fit parameters were used to simulate the uni-axial strain experiment analytically, the transverse stress was predicted to be tensile at relative volumes near lock-up. When the secant shear modulus values near lock-up were lowered a small amount, by lowering the coupling coefficient by twelve percent, and the other parameters were refit, the predicted transverse stress behaved physically and monotonically at all compressive levels and the predicted axial stress and shear modulus responses changed only slightly.

It is speculated that the shear modulus data around lock-up was artificially high due, in part, to how the experiment was analyzed. While the use of uni-axial strain may be appropriate for relative volumes near unity, it clearly is not valid for relative volumes around lock-up where the material behavior is nearly incompressible. Hence, it is speculated that as the relative volume approached lock-up, the ring expanded radially at both the inner and outer radii, and the specimen stiffness increased for geometrical reasons. Unfortunately, the experimental analysis assumed the increased stiffness was due entirely to material behavior and thus yielded artificially high shear modulus values near lock-up. While it is possible to simulate the combined compression/torsion experiment with finite elements and infer the parameter values via successive runs, a more productive approach is to develop a true uni-axial strain with torsion experiment – possibly with transverse stress instrumentation. This would greatly simplify and improve the experimental analysis and curve fitting process.

Appendix A

The polyconvexity of several candidate isotropic strain energy terms $\varphi(\mathbf{F})$ are investigated. All terms considered are functions of only the strain invariants $\overline{I}_1$ and J, and have real symmetric rank-two Hessian matrices, $\boldsymbol{H}$. For a rank two matrix, if $tr(\boldsymbol{H}) \geq 0$ and $Det(\boldsymbol{H}) \geq 0$, then $\boldsymbol{H}$ is positive semi-definite and its corresponding function is convex. (Recall, the trace of a matrix is the sum of its eigenvalues and the determinate is the product of its eigenvalues.) Attention is restricted to deformation gradients in which $J > 0$, and the fact that $\overline{I}_1 \geq 3$ is utilized. For completeness, it is assumed $\varphi(\mathbf{F}) = \infty$, when $J \leq 0$. As each potential can be multiplied by a positive constant without changing the results, the positive constant is dropped for simplicity.

I. Consider the term

$$\varphi = \frac{\overline{I}_1}{J^k} - 3$$

which, when expressed in terms of the deformation gradient, equals

$$\varphi = \frac{\|\mathbf{F}\|^2}{J^{k+2/3}} - 3 \, .$$

The trace and determinate of its Hessian matrix are

$$tr(H) = \frac{\overline{I}_1}{J^{k+2}}(k + 2/3)(k + 5/3) + \frac{2}{J^{k+2/3}}$$

and

$$Det(H) = \frac{-6\overline{I}_1}{J^{2k+8/3}}(k + 2/3)(k+1) \, ,$$

respectively. The trace is non-negative when $k \le -5/3$ or $k \ge -2/3$, while the *Det*(***H***) is non-negative when $-1 < k < -2/3$. Thus, the term is convex and polyconvex only when $k = -2/3$, i.e., $\varphi = I_1 - 3$. Note, this form is that of an incompressible neo-Hookean solid that Ball (1977) showed to be polyconvex.

II. Consider the term

$$\varphi = \frac{\bar{I}_1 - 3}{J^k}$$

which, when expressed in terms of the deformation gradient, equals

$$\varphi = \frac{\|\mathbf{F}\|^2 - 3}{J^{k+2/3}}.$$

The trace and determinate of its Hessian matrix are

$$tr(H) = \frac{1}{J^{k+2}}\left(2J^{4/3} + (k + \tfrac{2}{3})(k + \tfrac{5}{3})\bar{I}_1 - 3k(k+1)\right)$$

and

$$Det(H) = \frac{-2}{J^{2k+8/3}}\left(\bar{I}_1(k + \tfrac{2}{3})(1+3k) + 3k(k+1)\right),$$

respectively. The trace is non-negative when $k \ge -2/3$, and *Det*(***H***) is non-negative when $-2/3 \le k \le -1/3$. Hence, the function is convex and thus polyconvex when $-2/3 \le k \le -1/3$.

III. Consider the term

$$\varphi = \frac{(\bar{I}_1 - 3)^j}{J^k}$$

with positive *j* and *k* values. When expressed in terms of the deformation gradient, it equals

$$\varphi = \frac{\left(\dfrac{\|\mathbf{F}\|^2}{J^{2/3}} - 3\right)^j}{J^k}.$$

The trace and determinate of its Hessian matrix are

$$tr(H) = \frac{(\bar{I}_1 - 3)^{j-2}}{9J^{k+2}}(f_1 J^{4/3} + f_2)$$

and

$$Det(H) = \frac{2j(\bar{I}_1 - 3)^{2j-3}}{9J^{2k+8/3}} g,$$

respectively. Here

$$f_1 = 18j\left(\bar{I}_1(2j-1) - 3\right),$$

$$f_2 = 9k^2(\bar{I}_1 - 3)^2 + 3k(\bar{I}_1 - 3)\left(3(\bar{I}_1 - 3) + 4j\bar{I}_1\right) + 2j\bar{I}_1\left((3+2j)\bar{I}_1 - 15\right),$$

and

$$g = \bar{I}_1^2\left(8j^2 + 6j(k-1) - 9k(1+k)\right) - \bar{I}_1 6j(1+3k) + 81k(1+k)\ .$$

For all admissible values of J and $\bar{I}_1$, $f_1 \geq 0$ when $j \geq 1$, and $f_2 \geq 0$ when $j \geq 1$ and $k \geq 0$. Thus $Det(\boldsymbol{H})$ is non-negative when $j \geq 1$ and $k \geq 0$.

The term g equals zero when

$$j = (\frac{3}{8})\frac{12 + \Delta(7-3k) - \Delta^2(k-1) \pm \sqrt{(3+\Delta)^2\left(16 + \Delta^2(1+3k)^2 + 8\Delta(1+5k+6k^2)\right)}}{(3+\Delta)^2},$$

where $\Delta = \bar{I}_1 - 3$. (Note that since $\bar{I}_1 \geq 3$, $\Delta \geq 0$.) Since only non-negative values of j are sought, only the positive root is considered. For a given value of k, the maximum value of j occurs when $\partial j/\partial\Delta\big|_k = 0$, i.e., when $\Delta = 6\left(\dfrac{-2 \pm \sqrt{2}(1+3k)}{1+3k}\right)$. Let Δ^* denote the value of Δ at this point. Since Δ must be non-negative, Δ^* is defined as

$$\Delta^* = \max\left(0, \sqrt{2} - \frac{2}{1+3k}\right).$$

When j equals

$$j = (\frac{3}{8})\frac{12 + \Delta^*(7-3k) - \Delta^{*2}(k-1) + \sqrt{(3+\Delta^*)^2\left(16 + \Delta^{*2}(1+3k)^2 + 8\Delta^*(1+5k+6k^2)\right)}}{(3+\Delta^*)^2},$$

*Det(**H**)* is non-negative for all admissible values of $\bar{I}_1$.

For positive values of j and k, *tr(**H**)* and *Det(**H**)* are non-negative when

$$j \geq \max\left(1, (\frac{3}{8})\frac{12 + \Delta^*(7-3k) - \Delta^{*2}(k-1) + \sqrt{(3+\Delta^*)^2\left(16 + \Delta^{*2}(1+3k)^2 + 8\Delta^*(1+5k+6k^2)\right)}}{(3+\Delta^*)^2}\right)$$

A conservative approximation for this restriction is $j \geq k+1$. Hence, the term is convex and polyconvex when these conditions are satisfied.

7 References

Ball, J.M., "Convexity Conditions and Existence Theorems in Nonlinear Elasticity," *Archive for Rational Mechanics and Analysis*, **63**, #4, pp. 337-403, 1977.

Danielsson, M., Parks, D.M., and Boyce, M.C., "Constitutive Modeling of Porous Hyperelastic Materials," *Mechanics of Materials*, **36**, pp. 347-358, 2004.

Drucker, D.C., "A Definition of a Stable Inelastic Material", ASME Journal of Applied Mechanics, **26**, pp.101-195, 1959.

Ebbing, V., "Design of Polyconvex Energy Functions for All Anisotropy Classes," Ph.D. thesis, University Duisburg-Essen, Essen, 2010.

Gibson, L.J., and Ashby, M.F., **Cellular Solids**, 2nd Edition, Cambridge University Press, Cambridge, 1997.

Hartmann, S., and Neff, P., "Polyconvexity of General Polynomial-type Hyperelastic Strain Energy Functions for Near-incompressibility," *International Journal of Solids and Structures*, **40**, p. 2767-2791, 2003.

Lewis, M.W., "A Stable, Hyperelastic Model for Isotropic Foams", Los Alamos National Laboratory, Report LA-CP-07-0010, Los Alamos, 2005.

Miehe, C., "Aspects of the Formulation and Finite Element Implementation of Large Strain Isotropic Elasticity," *International Journal for Numerical Methods in Engineering*, **37**, p. 1981-2004, 1994.

Schroder, J., and Neff, P., "Application of Polyconvex Anisotropic Free Energies to Soft Tissues," Fifth World Congress on Computational Mechanics, Vienna, Austria, 2002.

Schroder, J., and Neff, P., "Invariant Formulation of Hyperelastic Transverse Isotropy Based on Polyconvex Free Energy Functions," *International Journal of Solids and Structures*, **40**, p. 401-445, 2003.

Simo, J.C., and Hughes, T.J.R., **Computational Inelasticity**, Springer, New York, 1998.

Zywicz, E. and Lin, J., "DYNA3D: A Nonlinear, Explicit, 3-Dimensional Finite Element Code for Solid and Structural Mechanics: Version 14.1," Lawrence Livermore National Laboratory, Livermore, California, LLNL-SM-659276, 2014.